Powder Technology 305 (2017) 673–678

Contents lists available at ScienceDirect

Powder Technology

journal homepage: www.elsevier.com/locate/powtec

Production of nickel matrix composites reinforced with carbide particles by granulation of fine powders and mechanical pressing

Maria Roseane P. Fernandes [a], Antonio Eduardo Martinelli [b,*], Aloisio Nelmo Klein [c], Gisele Hammes [c], Cristiano Binder [c], Rubens M. Nascimento [b]

[a] Universidade Federal da Paraíba, Department of Materials Engineering, Campus Universitário I, Jardim Cidade Universitária, CEP: 58051-900 João Pessoa, PB, Brazil
[b] Universidade Federal do Rio Grande do Norte, Department of Materials Engineering, Av. Salgado Filho 3000, Lagoa Nova, CEP 59.072-970 Natal, RN, Brazil
[c] Universidade Federal de Santa Catarina, Department of Mechanical Engineering, Caixa Postal 476, Campus Universitário, Trindade, CEP 88040-900 Florianópolis, SC, Brazil

ARTICLE INFO

Article history:
Received 2 June 2016
Received in revised form 23 September 2016
Accepted 29 October 2016
Available online 03 November 2016

Keywords:
Powder granulation
Nickel
Tantalum carbide
Niobium carbide
Metal matrix composite

ABSTRACT

Plain nickel and nickel composites containing either TaC or NbC powders were granulated and sintered after conventional mechanical pressing. The granulation parameters were studied using plain nickel powder to evaluate a binder system consisting of paraffin diluted in hexane, but also the suitable size range of the granules obtained. Carbide powders were then wet mixed with nickel and the powder mixtures were granulated using a drum. Flow rate tests were performed and the granules were pressed into pellets, which were dewaxed and sintered. SEM images of the microstructure of the sintered materials were obtained. Green and sintered densities along with Brinell hardness were also evaluated. The results revealed that the concentration of 1.5 wt% of paraffin and granules sieved in the range between 500 and 90 μm contributed towards the development of dense and uniform microstructures of the sintered composites. Finally, the addition of carbides homogeneously increased hardness to nearly double that of plain nickel.

1. Introduction

Powder granulation has been investigated for almost 70 years. Studies report the use of a variety of methods and equipment, including drums [1–2] applied to different materials, ranging from minerals to metallic powders of industrial interest [3]. Granulation has been extensively used to improve the flow rate of powders aiming at improved die feeding for mechanical pressing. High flow rates avoid defects such as mass heterogeneities in the green parts. Consequently, granulation yields homogenous density of pressed parts which results in dense and homogenous sintered products [4] characterized by superior physical characteristics and mechanical properties [5]. Granulation is especially recommended for fine powders, which normally exhibit low flow rates [6,7] and are difficult to handle and press using simple mechanical equipment. Defects originated from inappropriate die filling cannot be easily removed by further processing. Therefore, granulation is an important step to assure proper technological performance of sintered parts.

Powder granules are produced from a suspension of solid particles that agglomerate in a liquid phase [8–10]. The surface of the particles and the binding liquid must be of identical polarity [11–12]. The liquid binds the particles together by a combination of capillary pressure, surface tension, and viscous forces to a point where permanent solid bridges are formed after evaporation of the solvent [13–14]. Two attractive interparticle forces take place. Electrostatic forces are responsible for the initial agglomeration, however, they do not significantly contribute to the final strength of the granules, defined by van der Waals attraction, whose magnitude is usually four times higher [15,16]. Powder granulation is, in fact, an intricate process involving a number of simultaneous physical phenomena: i) wetting, nucleation and binder distribution; ii) consolidation and growth and iii) attrition and breakage [17–18]. A minimum amount of binder is determined by both powder and binder characteristics. Other important aspects of the process include binder distribution in the powder volume and time required for binder spreading [14]. The liquid-powder mixture is stirred to promote dispersion and growth of the granules, which are formed by the collision and adhesion of primary particles in discrete granules and/or growth around a core where the particles collide and aggregate to form layers.

Granulation can be performed in a drum. This method is especially useful to process small powder batches and to reduce production costs [19]. A binder and its solvent are added to the powder mixture and the batch is rotated in the drum. As the solvent evaporates, the particles coalesce in granules. The spreading efficiency of the binder solution is the main controlling feature of the process; however, binder selection for a particular powder system is quite often empirical [20].

* Corresponding author.
E-mail addresses: roseanef@gmail.com (M.R.P. Fernandes), martinelli.ufrn@gmail.com (A.E. Martinelli), a.n.klein@ufsc.br (A.N. Klein), gisele@emc.ufsc.br (G. Hammes), cristiano.binder@ufsc.br (C. Binder), rmaribondo@ufrnet.br (R.M. Nascimento).

http://dx.doi.org/10.1016/j.powtec.2016.10.053
0032-5910/

Final granule size distribution mainly depends on processing parameters such as residence time of particles in the drum and rotation speed [21].

Metal matrix composites (MMCs) can be manufactured by powder metallurgy (PM). Sintered parts have gained growing attention and achieved significant market expansion. An increasing number of sintered metallic components with improved performance and manufactured at low cost [22] has been successfully produced. PM involves a small number of energy efficient processing steps and results in near net shape parts with a wide variety of compositions and complex geometric shapes [23]. The production of MMCs with dispersed ceramic particles can be easily achieved by powder metallurgy [24]. The metallic matrices provide plasticity, whereas the dispersed ceramic particles adjust several target properties, such as hardness, strength and wear resistance. In addition, the porosity and pore size distribution of the sintered parts can be adjusted to result in either dense components or parts with porosity gradient, potentially expanding the number of applications for these materials.

Nickel is of great interest for its vast use in engineering applications that require some of its unique properties such as magnetism, strength, corrosion and wear resistance at high temperatures. In the latter case, improved properties can be achieved by adding dispersed hard particles such as TaC and/or NbC into Ni powder and sintering to nearly full density [25]. The main problem in the manufacture of composite parts with fine reinforcing ceramic particles is their distribution in the microstructure of the sintered component [26]. In order to obtain homogenous distributions, and therefore, little property variation along the microstructure, fine powders are preferable; therefore, granulation of the powder feedstock becomes important. In this scenario, the main goal of this work was the study the granulation of Ni-TaC and Ni-NbC powders to produce nickel-based sintered metal matrix composites by conventional powder metallurgy.

2. Materials and methods

2.1. Materials

The materials used were carbonyl nickel powder (D_{50} = 6.00 μm and ρ_{th} = 8.9 g/cm^3) provided by Epson Atmix Corporation (Japan), TaC (D_{50} = 2.18 μm and ρ_{th} = 13.9 g/cm^3) and NbC powders (D_{50} = 2.26 μm and ρ_{th} = 6.3 g/cm^3) supplied by H. C. Starck (Germany). SEM micrographs of the starting powders can be seen in Fig. 1. Commercially available paraffin lentils and hexane solvent were used to granulate the feedstocks.

2.2. Methods

The granulation parameters and the appropriate particle size range of the granules were initially studied. Granulation of plain Ni was performed using different contents of paraffin, i.e., 0.5, 1.0 and 1.5 wt%, diluted in hexane in ultrasound bath for 30 min in a sealed container. Subsequently, 100 g of powder was added to the solution, which was then transferred to a drum. The granulated powders were separated using 500–90 μm and 850–180 μm sieves. The granules were then pressed, sintered, and the density, microstructure and Brinell hardness of the resulting samples were characterized. After defining the adequate contents of paraffin and the adequate granule size distribution, different concentrations of TaC or NbC powders (Table 1) were wet mixed with Ni using ethanol and 200 g of steel spheres (diameter of 0.3 cm). Powder batches of 150 g were mixed during 1 h. After drying in an oven at ~70 °C for about 2 h, the powders were granulated using 1.5 wt% paraffin, and the granules were classified using 500 to 90 μm sieves.

Flow rate tests were carried out using the Hall funnel with orifice diameter of 0.20 in., according to ASTM B213-13 [27]. The granulated powders were pressed under 600 MPa in double-acting mode. To minimize the friction between die and green compacts, amide wax soaked

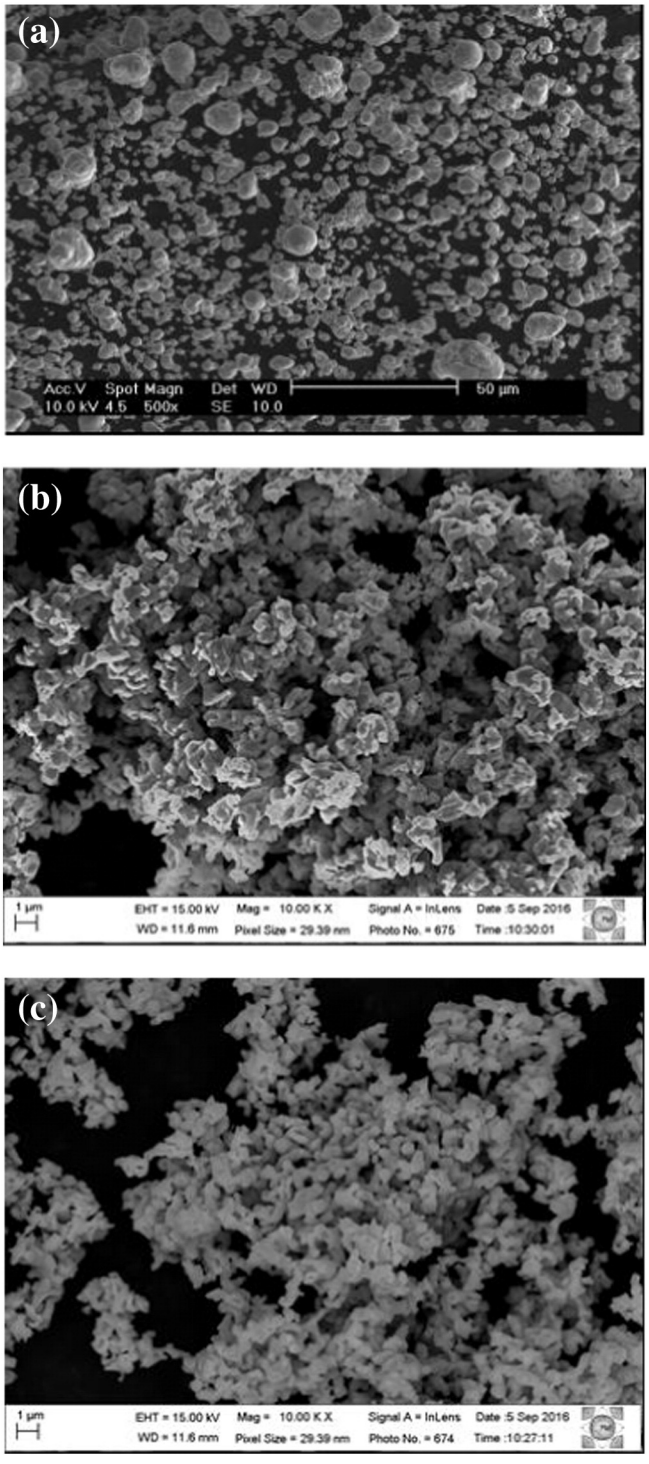

Fig. 1. SEM images of (a) Ni, (b) TaC and (c) NbC powders.

Table 1
Composite powder compositions and identification.

	N	NT5	NT10	NT15	NN5	NN10	NN15	NTN2.5	NTN5	NTN7.5
TaC										
(wt%)	0	5	10	15	0	0	0	2.5	5	7.5
(vol%)	0	3	6	10	0	0	0	2	3	5
NbC										
(wt%)	0	0	0	0	5	10	15	2.5	5	7.5
(vol%)	0	0	0	0	6	11	17	3	6	9

with alcohol was applied on the walls of the 10 mm diameter die. The geometric density of the green samples was measured using a decimal digit micrometer and a digital scale. The pellets were sintered in a conventional laboratory tube furnace. The heating rate from room temperature to 500 °C was 3 °C/min. After remaining 30 min at 500 °C for dewaxing, the samples were further heated at 8 °C/min up to the sintering temperature of 1150 °C. The holding time at that temperature was 1 h. A standard gas mixture of 95% Ar + 5% H_2 was used to prevent oxidation.

Brinell hardness measurements and microstructural analyses were carried out using samples mounted in bakelite and cut using a composite brass disc with diamond particles. The samples were polished with SiC paper (80, 120, 240, 400, 600, and 1200 mesh) and finished with 1.0 and 0.3 μm alumina slurries. Finally, the samples were etched in Marble solution and ultrasonically cleaned for about 5 min. An Emcotest set-up was used to measure the Brinell hardness of plain nickel and composite sintered samples. The primary load applied was 306.56 N during 5 s. Finally, SEM images of the microstructure were captured using a JEOL JSM 6390LV scanning electron microscope.

3. Results and discussion

3.1. Granulation and sintering plain nickel

SEM images of Ni powder granulated using different contents of paraffin are illustrated in Fig. 2. An analysis of the granules shown in the images, representative of the granulated powder, suggests that 1.5 wt% of paraffin resulted in roughly homogeneous granule size distribution and little fragmentation. Granules formed using either 0.5 or 1.0 wt% of paraffin did not reveal adequate resistance to handling. Further processing confirmed that they were susceptible to breakage into small fragments. At low binder concentrations, powder mixtures are not completely wetted by the solution, thus the production of large reliable granules with improved physical and mechanical properties is inefficient [28]. An adequate concentration of binder is required to form a liquid bridge between particles and high cohesive forces within the granules. These processes are controlled by granule fracture mechanisms. Additionally, high binder concentration increases the viscosity of the powder mixture [29]. Therefore, for the powder system studied, 1.5 wt% of paraffin combined with the viscosity of the binder resulted in adequate granule growth, with reasonable strength and fracture resistance. The flow rate is significantly lower for small granules, since the points of contact increase per unit volume. In addition, small granules adhere to the larger ones, resulting in irregularly shaped agglomerates [30], which affects packing and green density. Wetting is critical in defining uniform nuclei formation and, therefore, improved granule quality. Wide nuclei distributions often result in equally wide granule size distributions [31].

Although the concentration of paraffin affected the resistance to handling of the granules, it did not result in significant variation of the density of the sintered samples (Table 2). The final density obtained for samples containing 1.5 wt% of paraffin was 8.6 g/cm^3 with 3.4% porosity.

The microstructure of the sintered Ni samples granulated using different contents of paraffin is illustrated in Fig. 3. Although there is only a slight difference in the total porosity, pore size decreased with the increase in paraffin contents from 10 μm corresponding to 0.5 wt% of paraffin to 4 μm for 1.0 wt% of paraffin, and finally 2.5 μm for 1.5 wt% of paraffin. Pores are mainly concentrated is the grain boundaries, which can result in intergranular fracture.

The granulated powder is initially compacted by elastic-plastic deformation of the particles. In this stage, the contact areas between the particles are small and can be treated independently to a point where the packing density reaches 80% to 90% [32]. The porosity present in the sintered samples originates from granule packing flaws, especially related to of non-uniform granule size or shape (Fig. 2a and b) and frictional interactions that resulted in pressure gradients in the green

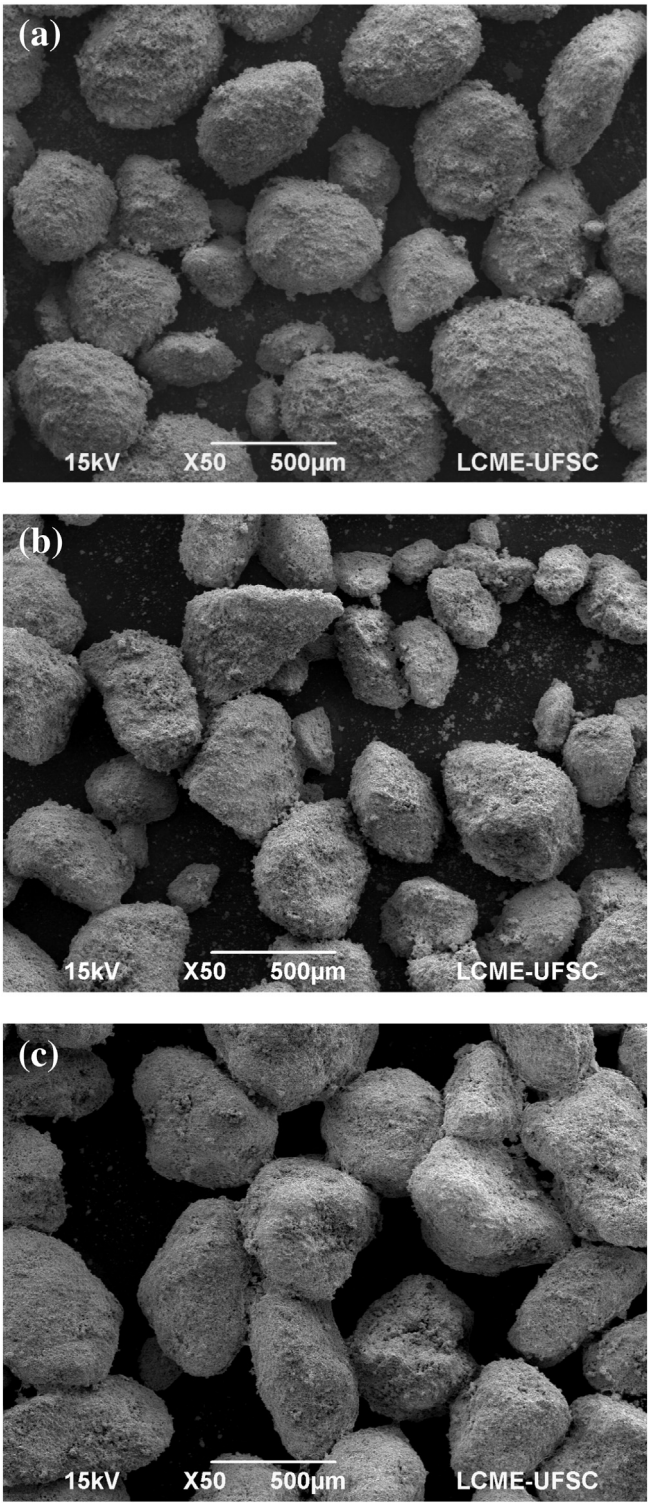

Fig. 2. Granules of fine Ni powder with (a) 0.5 wt%, (b) 1.0 wt% and (c) 1.5 wt% paraffin.

Table 2
Sintered density for different contents of paraffin and granule size range.

Concentration of paraffin (wt%)	$\rho_{sintered}$ (g/cm^3)/porosity 850–180 μm	$\rho_{sintered}$ (g/cm^3)/porosity 500–90 μm
0.5	8.4/5.6%	8.5/4.5%
1.0	8.5/4.5%	8.5/4.5%
1.5	8.5/4.5%	8.6/3.4%

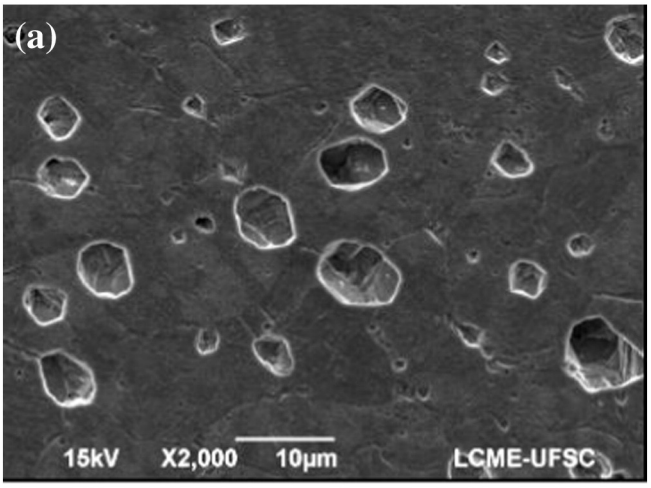

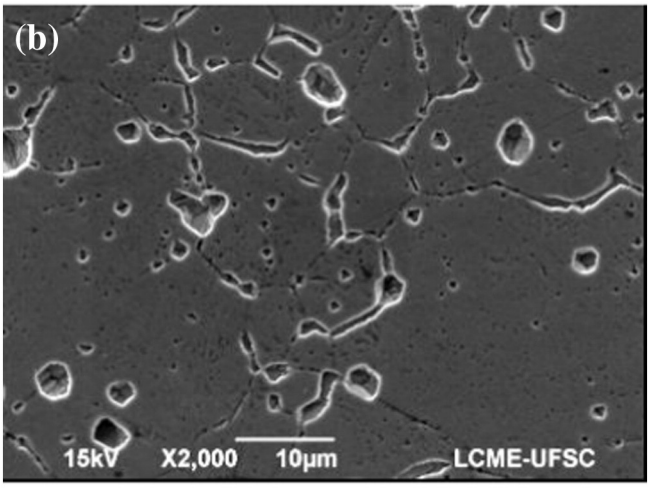

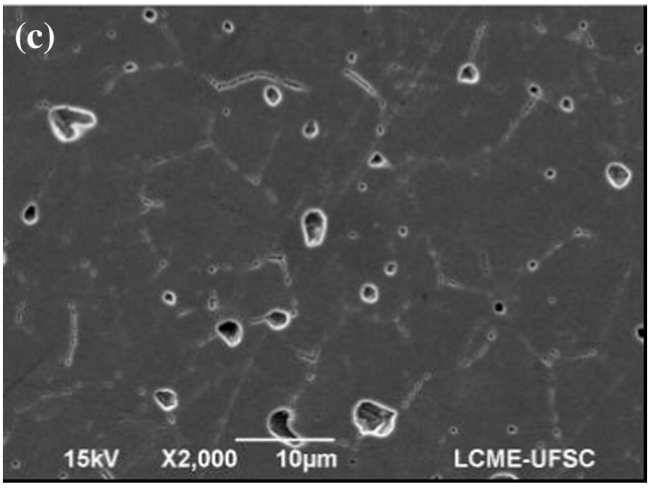

Fig. 3. SEM images of plain Ni sintered samples granulated using (a) 0.5%, (b) 1.0% or (c) 1.5% paraffin.

bodies [33]. Friction occurs both between the granules and the die wall and between powder particles within the granules. At early compaction stages, intergranular friction is dominant. At higher pressures, frictions at the die wall become more important. In the microstructure of sintered samples, residual primary pores between former powder particles could be observed as well as residual secondary pores between former granules.

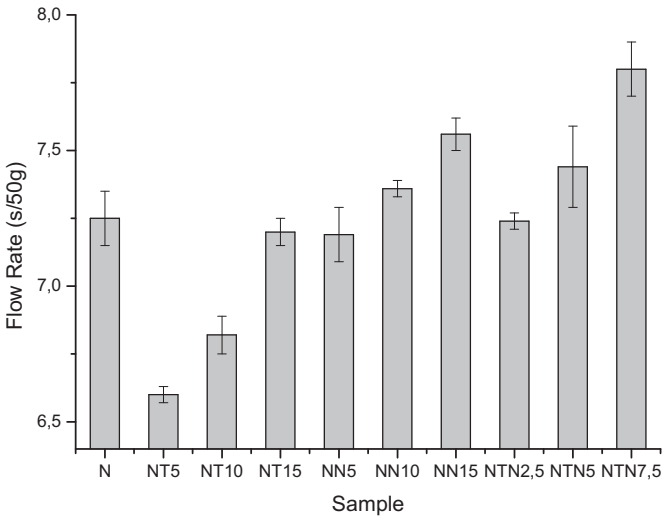

Fig. 4. Flow rate of granules with composite compositions.

3.2. Granulation and sintering composite compositions

The flow rate as a function of sample composition is shown in Fig. 4. It generally ranged from 6.5 to 7.7 s/50 g. The presence of TaC decreased the flow rate, whereas NbC increased it, as a result of the different densities of the powders. The density of TaC is 13.9 g/cm^3 whereas that of NbC is 6.3 g/cm^3. Denser granules flow easier. The difficulty encountered by Ni-NbC granules to flow in the Hall funnel was visible, especially for compositions NTN7.5 and NN15, which contained relatively high concentrations of NbC. In addition, the volume of powder in these samples was higher than that of the corresponding TaC compositions. Hence, additional paraffin would be necessary to provide better wetting of the particles.

Limited flow rates of powders containing 15 wt% carbide particles were noticed. This was a result of the large volume of powder to be granulated, which implies in higher concentration of paraffin. The maximum content of paraffin used in the scope of this work, i.e., 1.5 wt%, was not enough to fully wet some of the powder mixtures, i.e., NT15, NN15 and NTN7.5. Insufficient amount of paraffin increased the

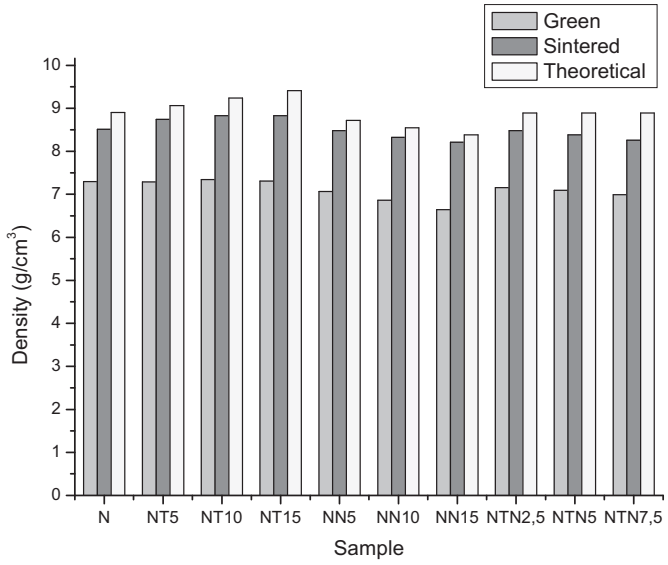

Fig. 5. Green, sintered and theoretical density of composite samples.

Table 3
Relative density of plain Ni and composite powders.

Composition	Green density (%)	Sintered density (%)
N	83	98
NT5	81	97
NT10	80	96
NT15	78	93
NN5	81	96
NN10	79	96
NN15	77	95
NTN2.5	81	96
NTN5	79	94
NTN7.5	78	92

interparticle friction and created a physical barrier between the non-granulated powder and the walls of the Hall funnel, preventing the powder from flowing freely. Additionally, the increase in fines, along with the presence of large granules increased interparticle attractive forces, which decreased particle-particle separation, thus reducing the flow rate. The interparticle forces that contribute to the cohesion of fine particles mainly include van der Waals forces, electrostatic forces, and capillary forces among other interfacial phenomena [34].

The green densities of the composite compositions are represented in Fig. 5. They ranged from 6.7 to 7.4 g/cm^3. TaC did not affect the green density, unlike the addition of NbC, which considerably decreased the density of the composite. This is due to the larger powder volume in the composite and the low density of NbC compared to that of the composite containing TaC and plain Ni. The volume of NbC in the powder mixture was basically double that of TaC. The relative density of the sintered samples can be seen in Table 3. There was a reduction in the relative density of the composites compared to plain Ni, as well as with the increase in the concentration of carbides. The lowest density values were obtained for compositions NT15 and NTN7.5, corresponding to the greater volume of carbides in the mixture, mainly NbC.

The density values of the sintered samples along with their theoretical density can be seen in Fig. 5. Overall, the sintered density ranged from 8.2 to 8.8 g/cm^3. Many compositions depicted nearly the full density of plain Ni, i.e., 8.9 g/cm^3. An example of a dense sintered microstructure is shown in Fig. 6, corresponding to the composite containing 10 wt% TaC homogenously dispersed along the Ni matrix.

Finally, Brinell hardness values of sintered nickel and nickel composites are shown in Fig. 7. The values are typical of sintered Ni and Fe-Ni alloys [35]. With the addition of TaC and NbC, hardness roughly doubled compared to that of plain Ni. Increasing the concentration of carbides also increased hardness. Moreover, an analysis of the standard deviation revealed little dispersion, attributed to homogeneous distribution of the carbides in the Ni matrix.

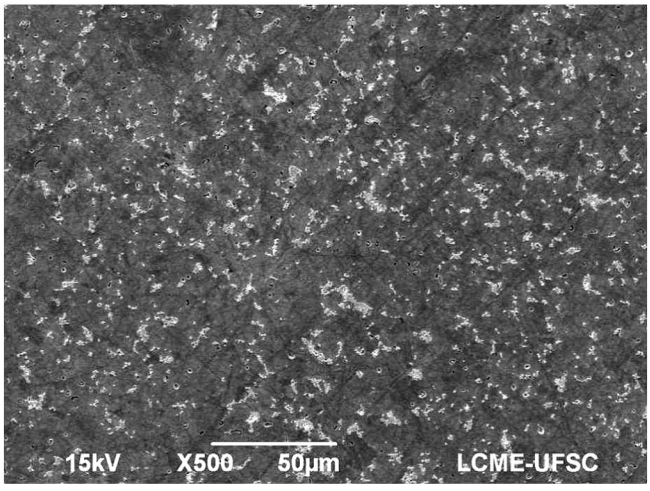

Fig. 6. SEM image of sintered NT10 sample.

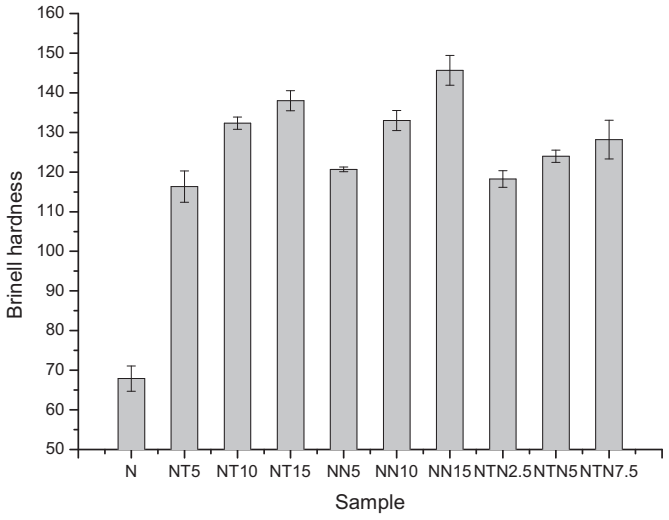

Fig. 7. Brinell hardness of plain Ni and Ni composites.

4. Conclusions

Ni and Ni composites with dispersed NbC or TaC particles were successfully sintered after granulation of the powder mixtures. A binder system consisting of paraffin (0.5 to 1.5 wt%) diluted in hexane was studied. Tests carried out for plain Ni established that the appropriate content of paraffin within the range investigated was 1.5 wt%. The resulting granules were sieved in the range of 500 and 90 μm, and displayed homogeneous size distribution and very little fragmentation. Although the total porosity of sintered plain Ni (3.4%) was not considerably affected by the concentration of paraffin used in the granulation, the pore size decreased as the concentration of paraffin increased. The pores were mainly observed in the grain boundaries of the Ni matrix. Ni-NbC and Ni-TaC powder mixtures were also granulated and sintered. The flow rate of the granulated composite mixtures ranged from 6.5 to 7.7 s/50 g. Differences in density of the carbide powders affected the flow rate of the composite. The addition of TaC decreased the flow rate, contrary to what was observed for NbC. High contents of carbides also reduced the flow rate, revealing that 1.5 wt% of paraffin was insufficient to wet large volumes of powder mixtures. Homogeneous composite microstructures with adequate dispersion of carbide particles could be obtained and depicted densities that ranged from 8.2 to 8.8 g/cm^3, whereas that of Ni is 8.9 g/cm^3. The addition of TaC and NbC proportionally increased the hardness of the composites to roughly double the hardness of plain Ni, with little variation along the surface of test samples, confirming the homogenous dispersion of the reinforcing carbide particles in the Ni matrix.

Acknowledgements

The authors would like to thank the Materials Laboratory - Labmat/UFSC, the Electron Microscopy Center Laboratory - LCME/UFSC for the use of their installations and CAPES/Brazil (PROEX 1948/2011) for its financial support.

References

[1] D.M. Newitt, J.M. Conway-Jones, A contribution to the theory and practice of granulation, Trans. I. Chem. Eng. 36 (1958) 422–441.

[2] C.E. Capes, P.V. Danckwerts, Granule formation by agglomeration of damp powders: part 1. The mechanism of granule growth, Trans. Inst. Chem. Eng. 43 (1965) 116–124.
[3] S.M. Iveson, J.D. Litster, K. Hapgood, B.J. Ennis, Nucleation, growth and breakage phenomena in agitated wet granulation processes: a review, Powder Technol. 117 (2001) 3–39.
[4] C. Mangwandi, L.J. Tao, A.B. Albadarin, S.J. Allen, G.M. Walker, Alternative method for producing organic fertilizer from anaerobic digestion liquor and limestone powder: High Shear wet granulation, Powder Technol. 233 (2013) 245–254.
[5] I.N. Tikhonova, A.M. Popov, N.V. Tikhonov, V.V. Tikhonov, Harnessing the capabilities of spray granulation in the food industry for the production of functional foods, Procedia Chem. 10 (2014) 419–423.
[6] N. Ku, C. Hare, M. Ghadiri, M. Murtagh, P. Oram, R.A. Haber, Auto-granulation of fine cohesive powder by mechanical vibration, Procedia Eng. 102 (2015) 72–80.
[7] J. Schmidt, M. Sachs, C. Blümel, B. Winzer, F. Toni, K. Wirth, W. Peukert, A novel process route for the production of spherical LBM polymer powders with small size and good flowability, Powder Technol. 261 (2014) 78–86.
[8] O.K. Semakina, S.A. Babenko, N.V. Vakhrameeva, Using of the agglomeration-in-liquid for the technology of the fine materials, Procedia Chem. 10 (2014) 305–309.
[9] J. Litster, B. Ennis, The Science and Engineering of Granulation Processes, Kluwer Academic Publishers, Dordrecht, 2004.
[10] N. Vlachos, I.T.H. Chang, Investigation of flow properties of metal powders from narrow particle size distribution to polydisperse mixtures through an improved Hall flowmeter, Powder Technol. 205 (2011) 71–80.
[11] D.A. Mota-Aguilar, C. Velázquez, Dynamics of the dry premixing stage of a hydrophobic formulation and potential implications on the wet granulation process, Powder Technol. 286 (2015) 318–324.
[12] O.K. Semakina, S.A. Babenko, N.V. Vakhrameeva, Using of the agglomeration-in-liquid for the technology of the fine materials, Procedia Chem. 10 (2014) 305–309.
[13] S.M. Iveson, P.A.L. Wauters, S. Forrest, J.D. Litster, G.M.H. Meesters, B. Scarlett, Growth regime map for liquid-bound granules: further development and experimental validation, Powder Technol. 117 (2001) 83–97.
[14] Siemens Westinghouse Power Corporation Pittsburgh, Pennsylvania, U.S.A. in: Y. Wen-Ching (Ed.), Handbook of Fluidization and Fluid-Particle Systems, CRC press, 2003.
[15] A. Hassanpour, C.C. Kwan, B.H. Ng, N. Rahmanian, Y.L. Ding, S.J. Antony, X.D. Jia, M. Ghadiri, Effect of granulation scale-up on the strength of granules, Powder Technol. 189 (2009) 304–312.
[16] L.J.L. Bernardes, A Granulação de Materiais, Cerâm. Ind. 11 (2006) 17–22.
[17] A.A. Adetayo, B.J. Ennis, Unifying approach to modeling granule coalescence mechanisms, Alche J. 43 (1997) 927–934.
[18] Y. Chen, J. Yang, R.N. Dave, R. Pfeffer, Granulation of cohesive Geldart group C powders in a Mini-Glatt fluidized bed by pre-coating with nanoparticles, Powder Technol. 191 (2009) 206–217.
[19] B.C. Xue, T. Liu, H. Huang, E.B. Liu, The effect of the intimate structure of the solid binder on material viscosity during drum granulation, Powder Technol. 253 (2014) 584–589.
[20] W.F. Sakr, M.A. Ibrahim, F.K. Alanazi, A.A. Sakr, Upgrading wet granulation monitoring from hand squeeze test to mixing torque rheometry, Saudi Pharm. J 20 (2012) 9–19.
[21] D. Barrasso, A. Tamrakar, R. Ramachandran, Model order reduction of a multi scale PBM-DEM description of a wet granulation process via ANN, Procedia Eng. 102 (2015) 1295–1304.
[22] A. Laptev, M. Bram, Manufacturing hollow titanium parts by powder metallurgy route and space holder technique, Mater. Lett. 160 (2015) 101–103.
[23] J. Park, S. Lee, S. Kang, J. Jeon, S.H. Lee, H. Kim, H. Choi, Complex effects of alloy composition and porosity on the phase transformations and mechanical properties of powder metallurgy steels, Powder Technol. 284 (2015) 459–466.
[24] C.P. Samal, J.S. Parihar, D. Chaira, The effect of milling and sintering techniques on mechanical properties of Cu–graphite metal matrix composite prepared by powder metallurgy route, J. Alloys Compd. 569 (2013) 95–101.
[25] M.R.P. Fernandes, A.E. Martinelli, A.N. Klein, C. Binder, G. Hammes, R.M. Nascimento, Plasma-assisted sintering TaC-NbC-Ni reinforced composites, Euro PM2014 - Sinter Steel Mechanical Properties, 2014.
[26] M.R.P. Fernandes, Compósitos de Matriz Metálica à base de Ni, 1. ed. Novas Edições Acadêmicas, Brazil, Saarbrücken, 2015 v.1 (156 pp.).
[27] ASTM B213-13, Standard Test Method for Flow Rate of Metal Using the Hall Flowmeter Funnel, 2013.
[28] M.X.L. Tan, K.P. Hapgood, Foam granulation: effects of formulation and process conditions on granule size distributions, Powder Technol. 218 (2012) 149–156.
[29] R.M. Dhenge, K. Washino, J.J. Cartwright, M.J. Hounslow, A.D. Salman, Twin screw granulation using conveying screws: effects of viscosity of granulation liquids and flow of powders, Powder Technol. 238 (2013) 77–90.
[30] J.L.A. Albero, A Operação de Prensagem: Considerações Técnicas e sua Aplicação Industrial Parte I: O Preenchimento das Cavidades do Molde, Cerâm. Ind. 5 (2000) 23–28.
[31] W.F. Sakr, M.A. Ibrahim, F.K. Alanazi, A.A. Sakr, Upgrading wet granulation monitoring from hand squeeze test to mixing torque rheometry, Saudi Pharm. J. 20 (2012) 9–19.
[32] E. Olsson, P.L. Larsson, A numerical analysis of cold powder compaction based on micromechanical experiments, Powder Technol. 243 (2013) 71–78.
[33] S. Cottrino, Y. Jorand, E. Maire, J. Adrien, Characterization by X-ray tomography of granulated alumina powder during in situ die compaction, Mater. Charact. 81 (2013) 111–123.
[34] A. Castellanos, The relationship between attractive interparticle forces and bulk behavior in dry and uncharged fine powders, Adv. Phys. 54 (2005) 263–376.
[35] J.S. Barboza, L. Schaeffer, L.L. Cerva, J.A.E. Lewis Jr., M.M. Dias, Comparative study of the mechanical properties of sinterized magnetic alloys applied to electrical machines' core, Powder Technol. 192 (2009) 12–15.